Lattice dynamics and external magnetic-field effects in Ni-Fe-Ga alloys

J. I. Pérez-Landazábal, V. Recarte, and V. Sánchez-Alarcos
Departamento de Física, Universidad Pública de Navarra, Campus de Arrosadía, 31006 Pamplona, Spain

J. A. Rodríguez-Velamazán
Instituto de Ciencia de Materiales de Aragón, CISC–Universidad de Zaragoza, 50009 Zaragoza, Spain and Institut Laue Langevin (ILL), 6 Rue Jules Horowitz, F-38042 Grenoble, France

M. Jiménez-Ruiz
Institut Laue Langevin (ILL), 6 Rue Jules Horowitz, BP 156, F-38042 Grenoble Cedex 9, Grenoble, France

P. Link
Forschungsneutronenquelle Heinz-Maier-Leibnitz (FRM-II), TU München, D-85747 Garching, Germany

E. Cesari
Departament de Física, Universitat de les Illes Balears, Ctra. de Valldemossa, km 7.5, E-07122 Palma de Mallorca, Spain

Y. I. Chumlyakov
Siberian Physical Technical Institute, Novo-Sobornaya Sq. 1, 634050 Tomsk, Russia
(Received 23 July 2009; revised manuscript received 16 September 2009; published 8 October 2009)

Precursor phenomena were investigated in a Ni-Fe-Ga alloy close to the stoichiometric Heusler composition Ni_2FeGa. In particular, the phonon-dispersion curves, the diffuse scattering and the magnetic properties of a single crystalline $Ni_{51.5}Fe_{21.5}Ga_{27}$ alloy were measured as a function of temperature. The TA_2 branch along the [110] direction of the $L2_1$ phase shows a significant phonon softening around $\xi=0.35$ resulting in a marked dip which becomes more pronounced as the temperature decreases. Diffuse neutron-scattering measurements performed along $[\bar{\xi}\xi 0]$ direction around Bragg reflections also reveal the presence of small satellite peaks at $\xi=0.33$ whose intensity increases on approaching the martensitic transformation temperature. Both elastic and inelastic-scattering anomalies confirm the occurrence of premartensitic phenomena in Ni-Fe-Ga alloys. The influence of an external magnetic field (6 T) on the anomalous phonon is shown to be negligible and just a small shift of the transformation temperature takes place because of the magnetic field.

DOI: 10.1103/PhysRevB.80.144301 PACS number(s): 63.20.−e, 64.60.−i, 81.30.Kf

I. INTRODUCTION

Several ferromagnetic Heusler alloys undergo a displacive martensitic transformation (MT) from a cubic $L2_1$-ordered phase ($Fm3m$ space group) to a low-temperature low-symmetry martensitic phase. The magnetic and vibrational behaviors near the structural martensitic transformation were widely reported in the literature in different alloy systems. In general, precursor phenomena occur prior to the MT (on cooling) of Heusler alloys, among them the diffuse elastic diffraction scattering along the [110] directions linked to structural modulations, the occurrence of a temperature-dependent dip of the acoustic TA_2-phonon branch at a wave vector inside the Brillouin zone (intracell distortion) and the softening of the long-wavelength limit of this acoustic TA_2-phonon branch at $q=0$ (softening of the C' shear modulus).[1–17]

Ferromagnetic shape memory alloys (FSMAs) were extensively studied during the last years because of the large magnetic-field-induced strains (MFIS) they show as a consequence of the field-induced reorientation of the crystallographic domains appearing below the thermoelastic MT. In particular, Ni-Fe-Ga alloys with compositions close to the stoichiometric Ni_2FeGa undergo a thermoelastic martensitic transformation on cooling from the Heusler $L2_1$-ordered phase at a critical point (T_m). Different martensitic phases are formed, namely, the modulated 5M, 6M, and 7M phases (having five-, six-, and seven-layered structures, respectively) or the nonmodulated 2M phase.[18–20] In a composition range, the transformation temperatures are below the Curie point (thus being possible candidates for MFIS) in such a way that during the MT both structural and magnetic changes occur simultaneously. Therefore, both magnetic and

TABLE I. Refined structural and magnetic parameters (300 K) corresponding to the $L2_1$ cubic phase obtained by single-crystal neutron diffraction.

$T=300$ K	Site	Atom	Occupancy
Lattice parameters (Å)	4*a* (0 0 0)	Fe	0.86(1)
$a=b=c=5.7495$		Ni	0.06(1)
		Ga	0.08(1)
	4*b* (0.5 0.5 0.5)	Ga	1.00(1)
	8*c* (0.25 0.25 0.25)	Ni	1.00(1)
	Magnetic moment (μ_B)	Fe	0.82(2)
		Ni	−0.07(2)
	χ^2		16.58

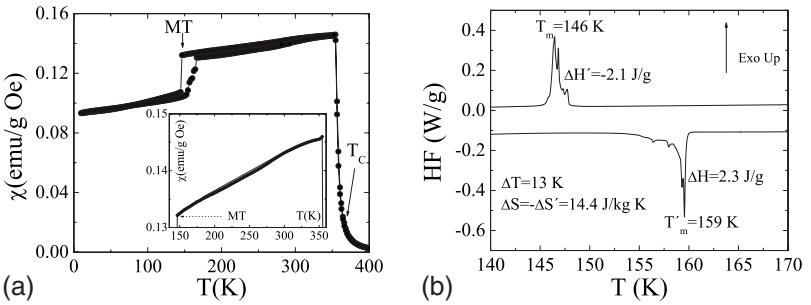

FIG. 1. (a) Temperature dependence of the real component of the magnetic susceptibility (χ) during a cooling-heating cycle (20 Hz and 3.5 Oe). (b) DSC measurements performed on cooling and heating at 10 K/min.

structural precursor phenomena could be present during cooling prior to the MT. Much effort was devoted in recent years to study the lattice dynamics previous to the MT in FSMA but most of them are focused on the Ni-Mn-Ga (Refs. 7–11) and Ni-Mn-Al (Refs. 14–16) and, more recently, on the Ni-Mn-In (Ref. 17) alloy systems. In this paper, the phonon-dispersion curves, the diffuse elastic scattering, and the magnetic properties of a single crystalline Ni-Fe-Ga alloy were measured as a function of temperature in order to analyze precursor phenomena previous to the MT. The magnetoelastic coupling was analyzed by determining the effect of the magnetic field on both the martensitic transformation and the precursor phenomena.

II. EXPERIMENTAL PROCEDURES

A $Ni_{51.5}$-$Fe_{21.5}$-$Ga_{27.0}$ (at. %) single crystalline alloy was prepared by the Bridgman technique. Several samples with convenient orientations were spark cut and homogenized under vacuum at 1420 K for 1 h and water quenched.

Rectangular parallelepipeds of $9\times4\times4$ mm^3 oriented with the edges parallel to the (100) directions were prepared for the neutron experiments (m=1.087 g). The phonon-dispersion curves and magnetic properties were measured as a function of temperature. The inelastic neutron-scattering experiments were performed on the triple-axis spectrometers IN3 (thermal neutrons) at the ILL (Institut Laue Langevin) and PANDA (cold neutrons) at FRM II (Forschungs-neutronenquelle Heinz-Maier-Leibnitz). Two different configurations were used on IN3: the pyrolytic graphite PG(002) monochromator and analyzer with fully open configuration for the low-energy excitations and the Cu(111) monochromator and PG(002) analyzer for the high-energy ones, both working at constant wave vector k_f=2.662 Å^{-1}. On PANDA, both monochromator and analyzer PG(002) crystals were used in the double focusing mode. A 6 cm PG filter was placed between the sample and the analyzer operation at fixed final wave vector k_f=1.97 Å^{-1}. The curves shown in the paper include both series of measurements.

Diffraction measurements were performed on the single-crystal D15 diffractometer (ILL). The instrument, provided with a closed-cycle cryostat, was used in the four-circle configuration at a wavelength of 1.173 Å. The nuclear and magnetic structures of the austenitic phase were studied at 300 K. The evolution of the precursor phase was monitored by carrying out q scans around several Bragg reflections along $[\xi\bar{\xi}0]$ direction at 5 K intervals between 320 and 160 K (always above T_m). At high temperature (320 K) the reflections observed were just those characteristic of the cubic Heusler structure (a=5.7495). On cooling, some small additional reflections appeared which could be indexed as $g\pm\xi$, where g is a reciprocal-lattice vector of the fcc lattice and $\xi\sim(1/3\ 1/3\ 0)$.

Differential scanning calorimetry (DSC) measurements at a heating/cooling rate of 10 K/min were carried out in a TA Q100 DSC to study the temperature-induced transformation. A Quantum Design MPMS XL-7 superconducting quantum interference device (SQUID) magnetometer[21] was used to measure the temperature dependence of the dc magnetization under different constant applied magnetic fields. The ac magnetic susceptibility was also experimentally detected under an exciting field amplitude H_{ac}=3.5 Oe at a frequency f=20 Hz.

III. RESULTS AND DISCUSSION

Since a nonstoichiometric alloy was used in the present study, a previous accurate crystallographic characterization of the simplest high-temperature austenitic phase was performed. Single crystal neutron diffraction was carried out in order to determine the occupancy factors of the different atomic positions corresponding to the austenitic $L2_1$ cubic

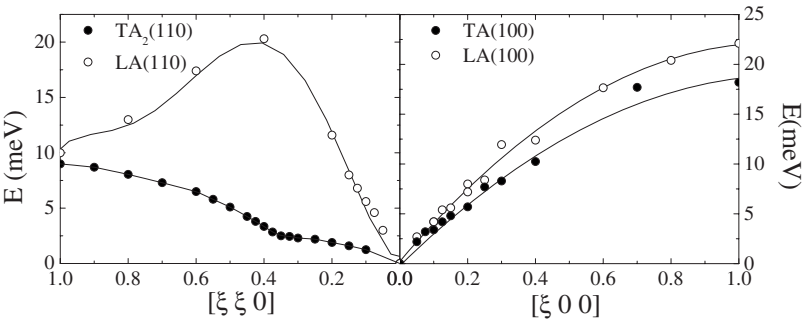

FIG. 2. Transversal (T) and longitudinal (L) phonon-dispersion curves measured along the high-symmetry directions $[\xi00]$ and $[\xi\xi0]$ at 300 K. The reduced wave-vector coordinate ξ is indicated in units of $2\pi/a$.

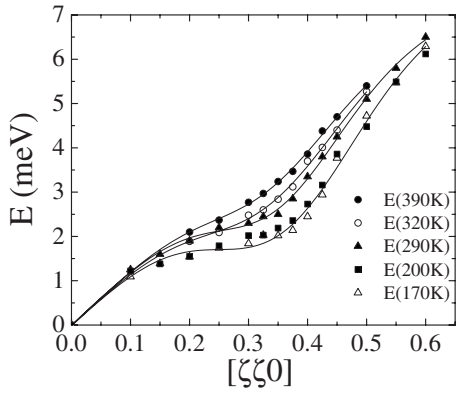

FIG. 3. Temperature dependence of the TA_2 phonon branch along the [110] direction of the $L2_1$ phase.

phase. The excess of Ni and Ga atoms redistribute in the Fe (000) positions. Table I summarizes the refined structural and magnetic parameters at 300 K. The magnetic response of the alloy is displayed in Fig. 1(a), where the temperature dependence of the real component of the magnetic susceptibility (χ) during a cooling-heating cycle is shown. The structural transition is accompanied, on cooling, by a decrease in the real susceptibility (and the corresponding increase on heating, see also the hysteretic behavior), which should be interpreted as a consequence of the lower magnetocrystalline anisotropy of the austenite phase as compared to the martensite. At higher temperatures, in austenite phase, the ferromagnetic transition occurs at $T_c=362$ K, which means that the MT occurs between ferromagnetic phases. A small and broad dip at higher temperatures between 185 and 295 K previous to the MT can also be appreciated in the susceptibility curve (see inset in Fig. 1). A similar behavior was observed in Ni-Mn-Ga alloys where the static modulation that appears previous to the MT has associated a drop in the susceptibility.[22] For these alloys, it was proposed that the modulated structure related to the soft $1/3[110]TA_2$-phonon mode[23] above the MT temperature may interact with the micromagnetic configurations already existing in the parent phase[13,24,25] below T_c and produce this characteristic behavior of the susceptibility. Nevertheless in the Ni-Fe-Ga system the anomaly in the magnetic susceptibility is much less well defined.

On the other side, Fig. 1(b) shows the DSC measurements performed on cooling and heating showing an exothermic peak at $T_m=146$ K corresponding to the forward MT and an endothermic one related to the reverse MT at $T'_m=159$ K. Different types of martensitic phases appear and coexist in Ni-Fe-Ga alloys with similar compositions[18–20] and this could be the cause of the jerky shape of the observed peaks. The enthalpy change in the forward transformation ($\Delta H' \approx -2.1$ J g^{-1} in absolute value) is slightly lower that the reverse one ($\Delta H \approx 2.3$ J g^{-1}). Nevertheless the forward and reverse transformation entropies are approximately the same ($-\Delta S' \approx \Delta S \approx 14.4$ J kg^{-1} K^{-1}). No premartensitic effects were observed by DSC.

The vibrational behavior of the austenitic $L2_1$ phase was analyzed through the phonon characteristics. Transversal and longitudinal phonon-dispersion curves measured along the high-symmetry directions [ξ00] and [$\xi\xi$0] at 300 K are shown in Fig. 2. The TA and LA curves along the [ξ00] direction do not show any anomaly. In contrast, both modes show a minimum and a maximum, respectively, for a particular wave-number ξ value along [$\xi\xi$0]. The elastic constants determined from the initial slope of the curves are $C_{11}=163\pm17$ GPa (LA in [ξ00]), $C_{44}=86\pm5$ GPa (TA in [ξ00]), $C_L=247\pm11$ GPa (LA in [$\xi\xi$0]), and $C'=13\pm2$ GPa (TA_2 in [$\xi\xi$0]). A striking feature of all measured phonon-dispersion curves in Heusler transforming shape memory alloys is the anomaly in the TA_2 branch along the [110] direction with polarization in [$1\bar{1}0$] direction. This mode has a minimum at a particular wave vector ξ depending on the structure of the approached martensitic phase.[11]

Focusing on the anomaly in the TA_2 branch along the [110] direction of the $L2_1$ phase, Fig. 3 shows its temperature dependence during cooling above the MT. The energies are equivalent to those reported in other alloy systems.[7–11] Significant phonon softening around $\xi=0.35$ is observed, resulting in a marked dip in the branch which becomes more pronounced as the temperature decreases. In the Ni-Mn-Ga case, the anomaly in the TA_2 branch was attributed to the Fermi-surface nesting along with strong electron-phonon coupling.[26] In the current case the dip is still present at 400 K, well above the Curie temperature indicating that the phonon anomaly is not related to the magnetic ordering.

Previous electron-diffraction results on stoichiometric Ni_2FeGa alloys[25,27] show diffuse satellite spots emanating from Bragg reflection along the [110] that correspond to micromodulated tweed structures. The experimental results suggest that the maximum intensity occurs at (1/3 1/3 0) positions. These diffuse satellites change progressively toward superstructures with lowering temperature. The simultaneous presence of 5M, 7M, and more complex superstructures in small areas was also observed below the MT temperature. To check this point elastic neutron scattering was performed as a function of temperature. Associated with the anomalous dip shown in the phonon-dispersion curves

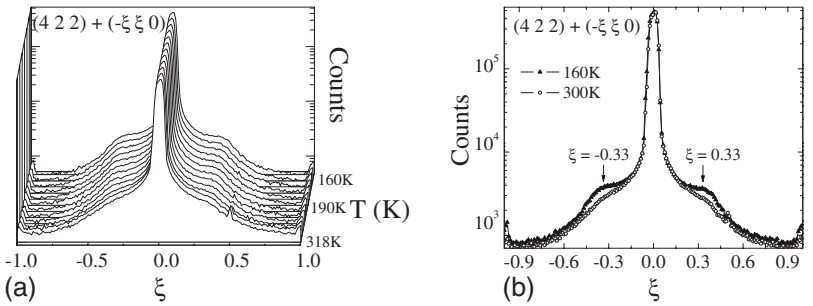

FIG. 4. (a) Temperature dependence of the elastic scattering along [$\bar{\xi}\xi$0] direction close to the (422) reflection. (b) Elastic scattering along [$\bar{\xi}\xi$0] direction close to the (422) reflection measured at 160 K (▲) and 300 K (○).

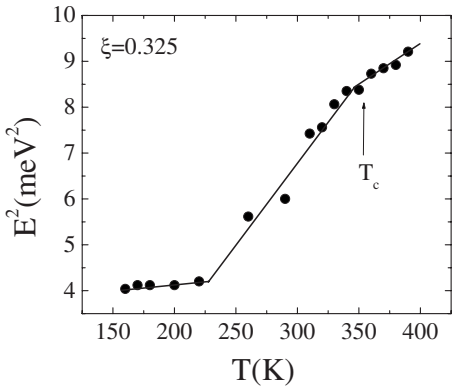

FIG. 5. Squared energy of the phonon at $\xi=0.325$ as a function of temperature.

Fig. 4(a) shows the temperature dependence of the elastic scattering along $[\bar{\xi}\xi 0]$ direction near the (422) reflection. A satellite peak develops close to $\xi=0.33$ whose intensity increases during cooling. To better compare the evolution of the satellites, Fig. 4(b) shows the elastic scattering at two different temperatures. These results are similar to those reported in Ni_2MnGa alloys although the intensity of the satellites appearing in Ni-Fe-Ga is quite lower.

The soft-mode frequency decreases as the temperature decreases but its energy remains finite in the analyzed temperature range. In accordance with experimental results in Ni-Mn-Ga and Ni-Al alloys, the squared energy of the phonon, E^2 at $\xi=0.325$ linearly decreases with temperature when approaching the MT as shown in Fig. 5. Nevertheless, below about 230 K the temperature dependence of the energy sharply varies. A similar (although more pronounced) change, leading to an anomalous increase in E^2 on cooling, was observed associated to the premartensitic transition taking place on Ni-Mn-Ga.[7,8] Therefore, the results suggest that the incomplete phonon anomaly observed in the Ni-Fe-Ga alloy must be linked to premartensitic phenomena. On the other side, the Curie temperature modifies the linear behavior of E^2 at high temperatures. This indicates an influence of the magnetic coupling on the premartensitic phenomena. In fact, as a result of the soft-mode evolution observed prior to the MT, the lattice becomes unstable and the atoms are displaced from their equilibrium positions. The amplitudes of the atomic thermal vibrations are enhanced so, the harmonic approximation does not hold. Then, an increase in the anharmonic contribution could modify the magnetoelastic coupling and change the magnetic and elastic behaviors of the alloy.[24] In this sense, the small and broad dip found between 185 and 295 K in the susceptibility curve (see inset in Fig. 1) can be linked to the incomplete TA_2 soft mode that appears in the same temperature range. As a consequence, the vibrational and magnetic properties are coupled in the stage previous to the MT.

To go deeper into the magnetic contribution (spin-phonon coupling), allowing to compare with previous results, the TA_2 branch along the [110] direction with transverse polarization was analyzed in a 6 T external magnetic field perpendicular to the scattering plane. Figure 6 shows the effect of the magnetic field at 170 and 290 K. In both cases the effect of the external magnetic field on the anomalous phonon is negligible, thus pointing out the scarce influence of the magnetic field on the vibrational precursor phenomena. Nevertheless, the different saturation magnetization of austenitic and martensitic phases hints to a probable shift in the MT temperature as a result of the application of the field. Figure 7 shows the temperature dependence of the magnetization at 0 and 6 T. The curves were measured in a heating cycle with the magnetic field applied along the [110] direction. In fact, the 0 T curve was measured in the remnant magnetic field of the SQUID system (around 13 Oe). The difference in magnetization at 6 T between the austenite and martensitic phases was estimated to be $\Delta M=-1.2$ A m^2 kg^{-1} at the transition temperature T_m. The derivative of both magnetization curves is shown in the inset of Fig. 7 in order to check the effect of the magnetic field in the transition temperature T_m. As shown, the magnetic field promotes a very small increase in the transition temperature. The shift between both curves allows to conclude that the temperature change corresponds to $dT_m/dB=70$ mK T^{-1}.

The shift of T_m with the applied magnetic field B can be evaluated on the basis of Clausius-Clapeyron equation. The equation is expressed as

$$\frac{dT_m}{dB}=-\frac{\Delta M}{\Delta S},$$

where ΔM is the difference in magnetization between the low-temperature martensitic phase and the high-temperature austenitic phase in the same applied magnetic field B. ΔS is the difference in entropy between both phases which can be considered independent of the field strength in this Ni-Fe-Ga alloys, similarly to Ni-Mn-Ga alloys.[11,28] Using the values determined in the previous results for $\Delta M=-1.2$ A m^2 kg^{-1} and $\Delta S=14.4$ J kg^{-1} K^{-1}, the deter-

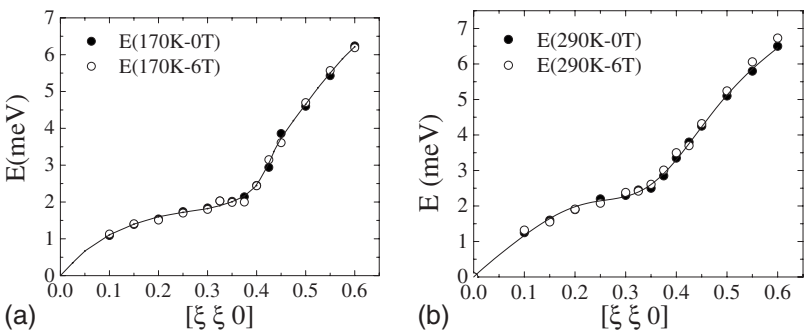

FIG. 6. TA_2 phonon branch along the [110] direction measured at (a) 170 K and (b) 290 K in a external field $H=0$ T (●) and $H=6$ T (○).

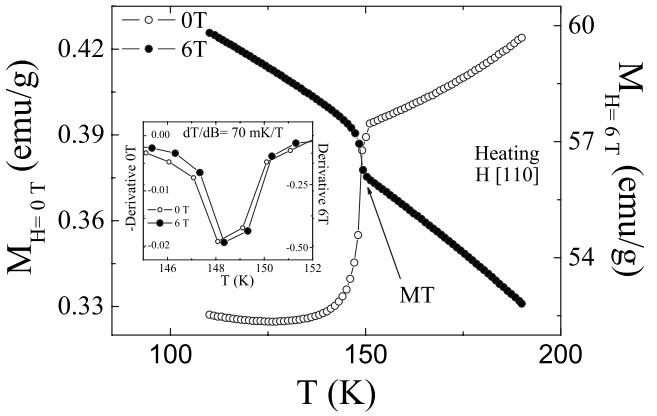

FIG. 7. Temperature dependence of the magnetization at 0 T (the remnant magnetic field of the squid is around 13 Oe) and 6 T. The magnetic field was applied along the [110] direction. The inset shows the derivative of both magnetization curves (the sign of the derivative at 0 T has been changed to better compare the curves).

mined value of $-\Delta M/\Delta S=83$ mK T^{-1} agrees quite well with the measured value of dT_m/dB.

IV. CONCLUSIONS

In summary, the TA_2 branch along the [110] direction of the $L2_1$ phase shows a significant phonon softening around $\xi=0.35$ resulting in a marked dip in the phonon branch which becomes more pronounced as the temperature decreases. The squared energy of the phonon decreases linearly with temperature but no complete vanishing is observed on approaching the martensitic transformation. Besides, elastic neutron scattering along $[\xi\bar{\xi}0]$ direction near to the (422) reflection shows a satellite peak close to $\xi=0.33$ whose intensity increases during cooling down to the MT temperature. These results reveal the occurrence of premartensitic phenomena in Ni-Fe-Ga alloys, similar to those already reported in the Ni-Mn-Ga system. On the other hand, the magnetoelastic coupling was analyzed by determining the effect of the magnetic field on both the martensitic transformation and the precursor phenomena. However, no significant magnetic-field influence was detected.

ACKNOWLEDGMENTS

This work was carried out with the financial support of the Spanish "Ministerio de Ciencia y Tecnología" and FEDER (Projects No. MAT2006-12838 and No. MAT2008-01587) and the Government of Navarra (Project entitled "Efecto magnetocalórico en aleaciones con memoria de forma ferromagnéticas"). This research project was also supported by the European Commission under the Sixth Framework Programme through the Key Action: Strengthening the European Research Area, Research Infrastructures under Contract No. RII3-CT-2003-505925. The Institute Laue Langeving (ILL), the Spanish CRG D15, and the Forschungsneutronenquelle Heinz-Maier-Leibnitz (FRM-II) are acknowledged for the allocated neutron beam time (Exp. INTER-118-IN3,CRG 1616-D15 and Exp. ID-1314-PANDA).

[1] V. V. Kokorin, V. A. Chernenko, E. Cesari, J. Pons, and C. Seguí, J. Phys.: Condens. Matter **8**, 6457 (1996).
[2] V. A. Chernenko, J. Pons, C. Seguí, and E. Cesari, Acta Mater. **50**, 53 (2002).
[3] E. Cesari, V. A. Chernenko, V. V. Kokorin, J. Pons, and C. Seguí, Acta Mater. **45**, 999 (1997).
[4] T. E. Stenger and J. Trivisonno, Phys. Rev. B **57**, 2735 (1998).
[5] Y. T. Cui, J. L. Chen, G. D. Liu, G. H. Wu, and W. L. Wang, J. Phys.: Condens. Matter **16**, 3061 (2004).
[6] Y. Ma, S. Awaji, K. Watanabe, M. Matsumoto, and N. Kobayashi, Appl. Phys. Lett. **76**, 37 (2000).
[7] A. Zheludev, S. M. Shapiro, P. Wochner, A. Schwartz, M. Wall, and L. E. Tanner, Phys. Rev. B **51**, 11310 (1995).
[8] A. Zheludev, S. M. Shapiro, P. Wochner, and L. E. Tanner, Phys. Rev. B **54**, 15045 (1996).
[9] L. Mañosa, A. Gonzalez-Comas, E. Obradó, A. Planes, V. A. Chernenko, V. V. Kokorin, and E. Cesari, Phys. Rev. B **55**, 11068 (1997).
[10] U. Stuhr, P. Vorderwisch, V. V. Kokorin, and P. A. Lindgard, Phys. Rev. B **56**, 14360 (1997).
[11] L. Mañosa, A. Planes, J. Zarestky, T. Lograsso, D. L. Schlagel, and C. Stassis, Phys. Rev. B **64**, 024305 (2001).
[12] V. Sánchez-Alarcos, J. I. Pérez-Landazábal, V. Recarte, C. Gómez-Polo, and V. A. Chernenko, Int. J. Appl. Electromagn. Mech. **23**, 93 (2006).
[13] J. I. Pérez-Landazábal, V. Sánchez-Alarcos, C. Gómez-Polo, V. Recarte, and V. A. Chernenko, Phys. Rev. B **76**, 092101 (2007).
[14] X. Moya, Ll. Maños, A. Planes, T. Krenke, M. Acet, O. Garlea, T. A. Lograsso, D. L. Schlagel, and J. Zarestky, Phys. Rev. B **73**, 064303 (2006).
[15] T. Mehaddene, J. Neuhaus, W. Petry, K. Hradil, P. Bourges, and H. Hiess, Mater. Sci. Eng., A **481-482**, 197 (2008).
[16] T. Mehaddene, J. Neuhaus, W. Petry, K. Hradil, P. Bourges, and A. Hiess, Phys. Rev. B **78**, 104110 (2008).
[17] X. Moya, D. González-Alonso, Ll. Mañosa, A. Planes, V. O. Garlea, T. A. Lograsso, D. L. Schlagel, J. L. Zarestky, S. Aksoy, and M. Acet, Phys. Rev. B **79**, 214118 (2009).
[18] K. Oikawa, T. Ota, Y. Tanaka, H. Morito, A. Fujita, R. Kainuma, K. Fukamichi, and K. Ishida, Appl. Phys. Lett. **81**, 5201 (2002).
[19] Y. Sutou, N. Kamiya, T. Omori, R. Kainuma, and K. Ishida, Appl. Phys. Lett. **84**, 1275 (2004).
[20] R. Santamarta, J. Font, J. Muntasell, F. Masdeu, J. Pons, E. Cesari, and J. Dutkiewicz, Scr. Mater. **54**, 1105 (2006).
[21] UNPN-E007 Feder Project, 2003.
[22] V. V. Khovailo, T. Takagi, A. D. Bozhko, M. Matsumoto, J. Tani, and V. G. Shavrov, J. Phys.: Condens. Matter **13**, 9655 (2001).
[23] T. Castan, A. Planes, and A. Saxena, Phys. Rev. B **67**, 134113 (2003).
[24] H. S. Park, Y. Murakami, D. Shindo, V. A. Chernenko, and T. Kanomata, Appl. Phys. Lett. **83**, 3752 (2003).

[25] J. Q. Li, Z. H. Liu, H. C. Yu, M. Zhang, Y. Q. Zhou, and G. H. Wu, Solid State Commun. **126**, 323 (2003).
[26] Y. Lee, J. Y. Rhee, and B. N. Harmon, Phys. Rev. B **66**, 054424 (2002).
[27] H. R. Zhang, C. Ma, H. F. Tian, G. H. Wu, and J. Q. Li, Phys. Rev. B **77**, 214106 (2008).
[28] J. Marcos, A. Planes, L. Mañosa, F. Casanova, X. Batlle, A. Labarta, and B. Martínez, Phys. Rev. B **66**, 224413 (2002).